

# Atmospheric Media Effects on ARIES Baseline Determination

S. C. Wu

Tracking Systems and Applications Section

*Large-scale atmospheric media increase apparent baseline length in ARIES baseline determination. Relying on the "self-calibration" of ionosphere in S-band observations may result in a baseline length error as large as 30 cm over a 200-km baseline. Up to 90 percent of such error can be removed through calibration by a crude ionospheric model.*

## I. Introduction

It is well known that for VLBI observations over a short baseline (~300 km or shorter) a large part of the media errors is common between the two ray paths and cancels upon differencing. Such "self-calibration" becomes more complete as the baseline length reduces. It has been a general practice in ARIES baseline determination to rely on such self-calibration of ionospheric effects. It is also "well known" that media effects degrade baseline solutions mainly in the vertical component. However, it is found through covariance analyses that the component most sensitive to media depends heavily upon the correlation, between the two stations, of the media effects. It is also found that relying on the cancellation of ionospheric delays between the two ray paths of VLBI observations at S-band results in a large error in baseline length determination.

This article provides a comparison among different types of media effects on ARIES baseline determination. The effectiveness of simple ionospheric calibration models are studied. To perform the covariance analysis, an ARIES observation sequence needs to be assumed. For the current purposes, the observation sequence is selected to be that of experiment 80D over the JPL/Goldstone baseline (~180 km). This experiment consisted of 96 observations over a period of ~25 hours on March 25 to 26, 1980.

## II. Atmospheric Media Error Models

We shall study the following five error models of atmospheric media corrupting ARIES baseline determination. Although these models are simple and idealized, their effects approach the average effects on actual ARIES observations.

### A. Homogeneous Troposphere

For a constant zenith delay of  $A_z$ , the differenced delay between the two ray paths is

$$\Delta\tau = A_z(1/\sin \gamma_1 - 1/\sin \gamma_2) \quad (1)$$

where  $\gamma_1$  and  $\gamma_2$  are the elevation angles. Such model applies to an uncalibrated average troposphere with  $A_z = 230$  cm.

### B. Locally Homogeneous Troposphere

This model assumes homogeneity of the troposphere with independent zenith delay at each station. Such a model accounts for the systematic delay error after a gross homogeneous effect on each site is independently calibrated. For a residual zenith *differenced* delay of  $A_z$ , the effect over the baseline is scaled by the average elevation factor to give

$$\Delta\tau = A_z \frac{1/\sin \gamma_1 + 1/\sin \gamma_2}{2} \quad (2)$$

An  $A_z$  of a few cm may exist.  $A_z = 3$  cm will be assumed for this study.

### C. Random Troposphere

This model accounts for random deviation of the troposphere from a homogeneous calibration model. Even though the effect is still elevation-angle dependent, it behaves as random noise from observation to observation and should be treated as such. The magnitude of this effect is

$$\Delta\tau = \left( \frac{A_{z,1}^2}{\sin^2 \gamma_1} + \frac{A_{z,2}^2}{\sin^2 \gamma_2} \right)^{1/2} \quad (3)$$

where  $A_z$  is the zenith deviation on each site.  $A_{z,1} = A_{z,2} = A_z = 2$  cm will be assumed.

### D. Global Ionosphere

This model assumes that a single model applies to both stations but scaled by factors according to the solar-zenith angle and the elevation angle at each station. Let  $f(X)$  be the solar-zenith angle factor and  $g(\gamma)$  the elevation angle factor, then

$$\Delta\tau = A_z [f(X_1)g(\gamma_1) - f(X_2)g(\gamma_2)] \quad (4)$$

where  $A_z$  is the zenith delay through the ionospheric peak and

$$f(X) = \begin{cases} 0.2 + 0.8 \cos^{2/3} X & X < 90 \text{ deg} \\ 0.2 & X > 90 \text{ deg} \end{cases} \quad (5)$$

$$g(\gamma) = 27[(1.071^2 - \cos^2 \gamma)^{1/2} - (1.034^2 - \cos^2 \gamma)^{1/2}] \quad (6)$$

During the period of experiment 80D, an independent Faraday rotation measurement indicated an ionospheric peak of  $\sim 8$  meters at S-band.  $A_z = 800$  cm will be assumed.

### E. Random Ionosphere

A random deviation from a global ionospheric model will result in a differenced delay between the two stations. The magnitude of the random delay error is

$$\Delta\tau = A_z \frac{f(X_1)g(\gamma_1) + f(X_2)g(\gamma_2)}{2} \quad (7)$$

where  $A_z$  is the rms differenced delay;  $f$  and  $g$  are as defined in Eqs. (5) and (6), respectively. It is estimated that the differenced delay may amount to 10 percent of the uncalibrated absolute effect for every 1000 km of baseline. Hence, across the 180-km JPL/Goldstone baseline of experiment 80D,  $A_z = 14$  cm.

## III. Baseline Determination Errors

To estimate the effects of the media error models outlined in Section II, covariance analyses following Ref. 1 were performed. The solved-for parameters include three baseline components, epoch offset, and frequency offset. The effects of models A, B, and D are treated as systematic errors; those of models C and E are treated as random errors. All the 96 observations are included in a single estimation process. Table 1 summarizes the estimated baseline component errors from the above five types of media errors. It is observed that the "well-known" belief that the baseline *vertical* is most sensitive to media errors is valid only when the errors are uncorrelated (or negatively correlated) between the two stations. When the errors are correlated, as in the cases of homogeneous troposphere and global ionosphere without calibrations, it is the baseline *length* that is most affected. In other words, a media model that is common to both stations and that tends to cancel upon differencing will give rise to an error mainly in baseline length.

The above unexpected results can be visualized, at least in the case of homogeneous troposphere, by the following reasoning. The information of baseline length is extracted mainly from delay observations nearly parallel to the baseline. The delay due to a homogeneous troposphere is always longer for the lagging station due to lower elevation angle as a result of the spherical earth surface. Hence the apparent baseline is always longer than its true value. For the other two components, the information is extracted mainly from delay observations nearly perpendicular to the baseline. The elevation angles and thus the delays due to a homogeneous troposphere are nearly the same for the two stations. Hence baseline components perpendicular to the length are hardly affected.

It should be pointed out that the effects of a homogeneous troposphere can be easily calibrated. This is routinely done in ARIES data processing. It is included in the above study simply for comparison and completeness.

An uncalibrated ionospheric effect appears to be a significant error source (at S-band) in the determination of baseline

length. To examine the modeling effects of the global ionosphere, two smooth models

$$f(X) = 0.2 + 0.8 \cos^4(X/2) \quad (8)$$

and

$$f(X) = 0.2 + 0.8 \cos^2(X/2) \quad (9)$$

are also studied in place of Eq. (5). These three models are shown in Fig. 1. The resulting baseline errors due to a global ionospheric error following these three models are summarized in Table 2. The errors in baseline length do not show appreciable differences from one model to another. Hence ionospheric modeling cannot be condemned for the large error in baseline length. The above global ionospheric effect on baseline length was estimated for a 180-km baseline between JPL and Goldstone. This error increases with baseline length: For the 336-km baseline between JPL and OVRO, the baseline length error becomes 49.5 cm. Hence ionospheric calibration for ARIES S-band observations is deemed essential.

#### IV. Calibration of Ionospheric Effects

Since most ARIES experiments have been carried out at S-band only, S-X calibration is out of the question. An alternative is to make use of Faraday rotation data from Goldstone viewing one of the geostationary satellites. Daily records of these data have been, and continue to be, collected by the Tracking System Analytic Calibration (TSAC) Team. However, since the Faraday rotation measurements are taken at a single station by viewing a fixed ray path (with respect to the station), mappings need to be done before the data can be applied to other stations and ray paths. At present, such mappings are routinely performed by the TSAC Team on ray paths that view deep-space probes near the ecliptic plane. On the other hand, ARIES experiments include observing sources at high declination angles, the mappings to which are out of the current TSAC mapping limit.

Other handy information recorded by the TSAC Team is the zenith total electron content (TEC) plots. The peak value and the night-time value of the TEC on each day can easily be read out from these plots. A simple mapping scheme can be used to generate point-by-point calibration from the peak and the night-time TEC during any particular day when ARIES is taking observations.

To examine how an imperfect mapping will degrade the calibration, simulation analyses are performed. A "true" TEC as a function of solar-zenith angle  $X$  is assumed to be

$$E(X) = \begin{cases} E_{min} + (E_{max} - E_{min}) \cos^{2/3} X & X < 90 \text{ deg} \\ E_{min} & X > 90 \text{ deg} \end{cases} \quad (10)$$

The following four imperfectly mapped calibrations are examined:

- (1)  $E(X) = E_{min} + (E_{max} - E_{min}) \cos^4(X/2)$
- (2)  $E(X) = E_{min} + (E_{max} - E_{min}) \cos^2(X/2)$
- (3) Same as (1) with the peak shifted by 30 deg to the east from the sub-Sun point ( $X = 0$ ).
- (4) Same as (1) with the peak shifted by 15 deg to the north from the sub-Sun point ( $X = 0$ ).

The assumed "true" ionospheric TEC as a function of  $X$  is shown in Fig. 1 as a solid line for  $E_{max} = 1$  and  $E_{min} = 0.2$ . The calibrations of (1) and (2) above are shown in the same figure as a dotted line and a dash-dotted line, respectively. Table 3 summarizes the residual baseline errors due to imperfectly mapped calibrations. Here,  $E_{max}$  and  $E_{min}$  have been chosen to be equivalent to the 800-cm and 160-cm delays, which occurred on March 25 to 26, 1980 (Experiment 80D of ARIES). For comparison, the baseline errors without calibration are also shown. These results indicate that, except for model (2), all calibration models remove 90 percent of the baseline length error or better. In other words, to remove 90 percent of the ionospheric effects, the "shape" of the mapping function is allowed to be moderately imperfect, and the peak to be shifted by 30 deg in longitude or by 15 deg in latitude. Even the badly "out-of-shape" mapping of model (2) removes 70 percent of the baseline length error. Such high-degree removal of the global ionospheric effect is the result of decorrelating the effects between the two stations; the systematic effect is thus somewhat randomized and less corrupting on baseline length.

#### V. Conclusion

In baseline determination by the VLBI technique, the sensitivities of baseline components to atmospheric media effects depend heavily upon the correlation between the two ends of the baseline. The global-type media tends to affect mainly the baseline length. The effects are such as to lengthen the estimated baseline. High-degree removal of such ionospheric effects is possible even with a crude model, providing correct diurnal peak and minimum ionospheric levels are input. Uncalibrated ionospheric effects may result in an error of tens of centimeters at S-band over a baseline of 100 km or longer.

## Acknowledgment

The information for Faraday rotation measurement is provided by H. N. Royden and T. E. Litwin of TSAC Team.

## Reference

1. Wu, S. C., "Error Estimation for ORION Baseline Vector Determination", *TDA Progress Report 42-57*, Jet Propulsion Laboratory, Pasadena, Calif., June 15, 1980, pp. 16-31.

**Table 1. Media effects on JPL/Goldstone baseline determination**

| Media error model               | Value of $A_z$ , cm | Baseline component errors, cm |         |          |
|---------------------------------|---------------------|-------------------------------|---------|----------|
|                                 |                     | Length                        | Lateral | Vertical |
| Homogeneous troposphere         | 230                 | 28.0                          | 2.9     | 2.4      |
| Locally homogeneous troposphere | 3                   | 0.1                           | 0.5     | 8.9      |
| Random troposphere              | 2                   | 1.0                           | 1.1     | 2.4      |
| Global ionosphere               | 800                 | 26.5                          | 3.4     | 1.3      |
| Random ionosphere               | 14                  | 1.3                           | 1.3     | 2.8      |

**Table 2. Global ionospheric effects on JPL/Goldstone baseline determination**

| Media model | Value of $A_z$ , cm | Baseline component errors, cm |         |          |
|-------------|---------------------|-------------------------------|---------|----------|
|             |                     | Length                        | Lateral | Vertical |
| Eq. (5)     | 800                 | 26.5                          | 3.4     | 1.3      |
| Eq. (8)     | 800                 | 25.8                          | 1.1     | 2.5      |
| Eq. (9)     | 800                 | 33.7                          | 1.2     | 0.4      |

**Table 3. Residual ionospheric effects on JPL/Goldstone baseline determination**

| Calibration model | Baseline component errors, cm |         |          |
|-------------------|-------------------------------|---------|----------|
|                   | Length                        | Lateral | Vertical |
| No Calibration    | 26.5                          | 3.4     | 1.3      |
| Model (1)         | 0.7                           | 2.3     | 1.3      |
| Model (2)         | 7.2                           | 4.6     | 0.9      |
| Model (3)         | 1.0                           | 5.1     | 3.1      |
| Model (4)         | 2.9                           | 1.3     | 1.3      |

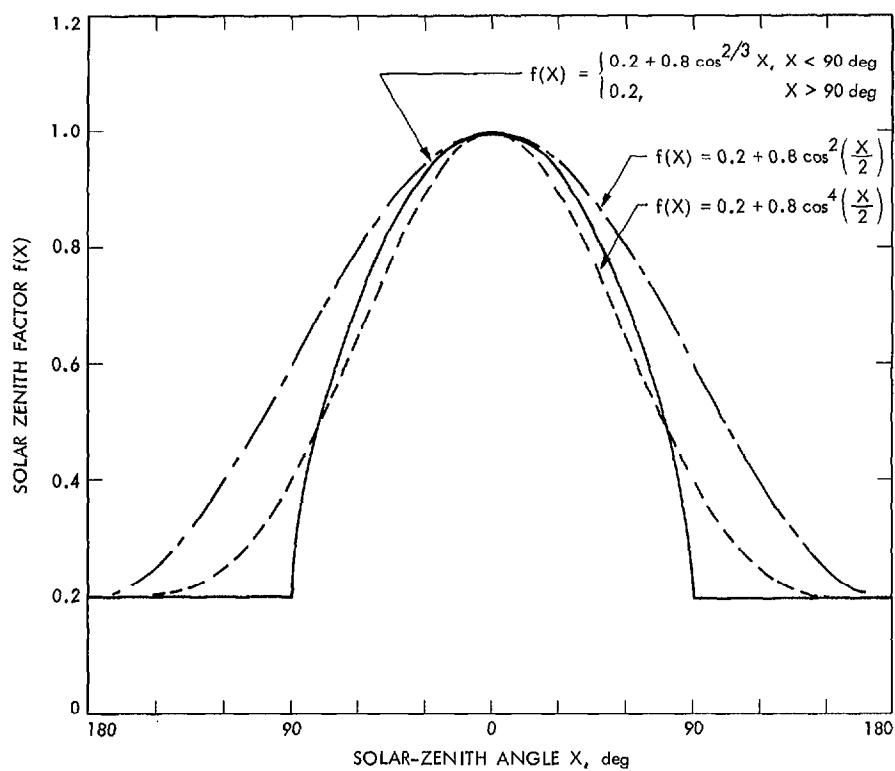


**Fig. 1. Solar-zenith angle factors of global ionospheric models**